Distortion/interaction analysis of the reactivities and selectivities of halo– and methoxy–substituted carbenes with alkenes

C. Avery Sader and K. N. Houk*

Department of Chemistry and Biochemistry, University of California, Los Angeles, California 90095 –1569, U. S. A.

E-mail: houk@chem.ucla.edu

Dedicated to Pierre Vogel, a great scientist and friend, on his 70th birthday

DOI: http://dx.doi.org/10.3998/ark.5550190.p008.408

Abstract

The transition structures for the (2+1) cycloadditions of dichlorocarbene, chlorofluorocarbene, and difluorocarbene to cyclohexene, 1–hexene, ethylene, and α–chloroacrylonitrile were located using quantum mechanical methods (M06–2X). In addition, transition structures for the (2+1) cycloadditions of chloromethoxycarbene, fluoromethoxycarbene, and dimethoxycarbene to ethylene and α–chloroacrylonitrile were computed. Except for the reactions with ethylene, these cycloadditions were studied experimentally and computationally by Moss and Krogh–Jespersen (Zhang, M.; Moss, R. A.; Thompson, J.; Krogh–Jespersen, K. *J. Org. Chem.* 2012, *77*, 843–850). As a complement to the work of those groups, we have utilized the distortion/interaction model to understand reactivities and selectivities. Gas–phase calculations were carried out at the M06–2X/6–31+G(d,p) level of theory.

Keywords: Carbenes, cycloadditions, distortion interaction model, density functional theory

Introduction

The cycloadditions of carbenes to alkenes constitute a general method for synthesis of cyclopropane ring structures. These cycloadditions have excited widespread interest in the mechanistic details of this reaction. Hoffmann predicted that a C_{2v} cyclic four–electron transition state in which both C–C bonds form simultaneously is orbital–symmetry forbidden;[1,2] therefore, non–least motion approach was proposed by Hoffmann[2] and Moore[3] in which there is initial interaction of the electrophilic empty *p*–orbital (LUMO) of the carbene with the nucleophilic filled π–orbital (HOMO) of the alkene.[1] This prediction was subsequently verified many times with semiempirical[4–6] and ab initio methods[7,8] and was shown to be influenced by a second pair of orbital interactions between the lone pair (HOMO) of the carbene with the π* antibonding

orbital (LUMO) of the alkene, which becomes dominant for electron-donor substituted carbenes.[8]

Carbene cycloadditions have been extensively studied experimentally and computationally by the groups of Moss and Krogh–Jespersen over the last decade.[9–12] They combined laser flash photolysis and density functional theory calculations to determine activation parameters for a series of carbene cycloadditions.[13] They found that trends in $\Delta E^{\ddagger}$ parallel expectations based on considerations of carbene stability and nucleophilicity. As a complement to the work of those groups, we have computationally investigated the (2+1) cycloadditions of dihalocarbenes **1a-c** to cyclohexene (**2a**) and 1-hexene (**2b**), as well as the cycloadditions of **1a-c** and methoxycarbenes **1d-f** to ethylene (**2c**) and α–chloroacrylonitrile (**2d**) in the context of the distortion/interaction model of reactivity developed by our group[14] (or the activation–strain model developed independently by Bickelhaupt).[15]

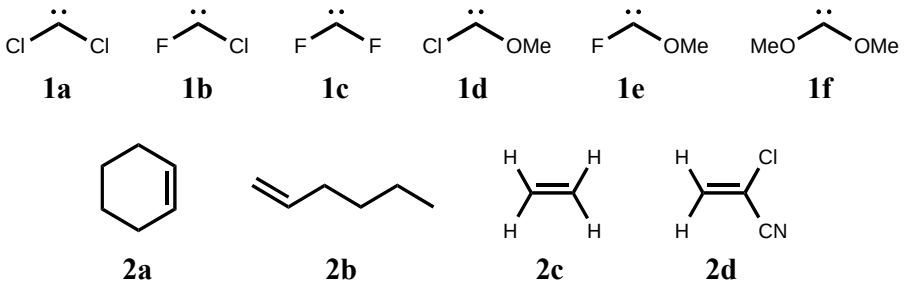

Figure 1. The carbenes and alkenes employed in this computational study. All except **2c** have been studied experimentally and computationally by Moss and Krogh–Jespersen.[13]

Computational Methodology

Gas phase reactant, product, and transition state geometry optimizations as well as analytical frequencies were computed using the hybrid meta–GGA functional M06–2X[16] with the 6–31+G(d,p) basis set in the Gaussian 09 suite of programs.[17] Tight convergence criteria and an ultrafine integration grid were used in all optimizations. All reactants have positive definite Hessian matrices and all transition structures have only one negative eigenvalue in their diagonalized force constant matrices. Intrinsic reaction coordinate (IRC)[18,19] calculations were performed to obtain a potential energy surface for distortion/interaction analysis and to ensure that all optimized transition structures connect the appropriate reactants and products.

Results and Discussion

The distortion/interaction model developed by our group has recently been applied to explain the reactivities and selectivities of (3+2) cycloadditions.[14] This model dissects activation barriers

($\Delta E^{\ddagger}$) of bimolecular reactions into distortion energies ($\Delta E_d^{\ddagger}$) and interaction energies ($\Delta E_i^{\ddagger}$). The distortion energy is the amount of energy required to distort the carbenes and alkenes into their transition state geometries without allowing the cycloaddition partners to interact. The interaction energy arises from a combination of closed–shell repulsion, charge transfer involving occupied and vacant orbital interactions, electrostatic interactions, and polarization effects. By definition, $\Delta E^{\ddagger} = \Delta E_d^{\ddagger} + \Delta E_i^{\ddagger}$, and the position of the transition state occurs at the point along the reaction coordinate, ζ, where the derivatives of the distortion and interaction energies are equal and opposite ($\delta\Delta E_d(\zeta)/\delta\zeta = -\delta\Delta E_i(\zeta)/\delta\zeta$). Figure 2 shows the transition structures for the cycloadditions of **1a–c** with **2a** and **2b** and **1a–f** with **2c** and **2d** computed with M06–2X/6–31+G(d,p). Table 1 shows the activation and total distortion energies, the contributions to the distortion energies of the carbene and the alkene, and the interaction energies for reactions of **1a–c** with **2a** and **2b** and **1a–f** with **2c** and **2d**.

Table 1. Distortion/interaction energies (in kcal mol^{-1}) for cycloaddition transition structures computed at the M06–2X/6-31+G(d,p) level

Carbene	Alkene	$\Delta E^{\ddagger}$	$\Delta E_d^{\ddagger}$ total	$\Delta E_d^{\ddagger}$ carbene	$\Delta E_d^{\ddagger}$ alkene	$\Delta E_i^{\ddagger}$
CCl_2	c–Hex	–4.1	2.6	1.5	1.1	–6.7
CClF	c–Hex	–1.3	5.3	2.0	3.3	–6.6
CF_2	c–Hex	7.4	9.2	2.6	6.6	–1.8
CCl_2	1–Hex	–3.3	1.5	0.9	0.6	–4.8
CClF	1–Hex	–0.9	3.4	1.5	1.9	–4.3
CF_2	1–Hex	6.4	7.3	2.0	5.3	–0.9
CCl_2	C_2H_4	0.1	1.7	0.8	0.9	–1.6
CClF	C_2H_4	3.3	3.1	1.2	1.9	0.2
CF_2	C_2H_4	10.3	5.8	1.5	4.3	4.5
ClCOMe	C_2H_4	8.4	6.9	3.4	3.5	1.5
FCOMe	C_2H_4	13.1	8.7	3.5	5.2	4.4
$C(OMe)_2$	C_2H_4	16.2	10.3	3.3	7.0	6.0
CCl_2	α–ClACN	–3.2	1.3	0.0	1.3	–4.5
CClF	α–ClACN	0.0	2.5	0.2	2.3	–2.5
CF_2	α–ClACN	5.4	5.0	0.4	4.6	0.3
ClCOMe	α–ClACN	0.0	4.8	0.9	3.9	–4.8
FCOMe	α–ClACN	3.4	6.1	1.0	5.1	–2.7
$C(OMe)_2$	α–ClACN	1.2	7.9	2.3	5.6	–6.7

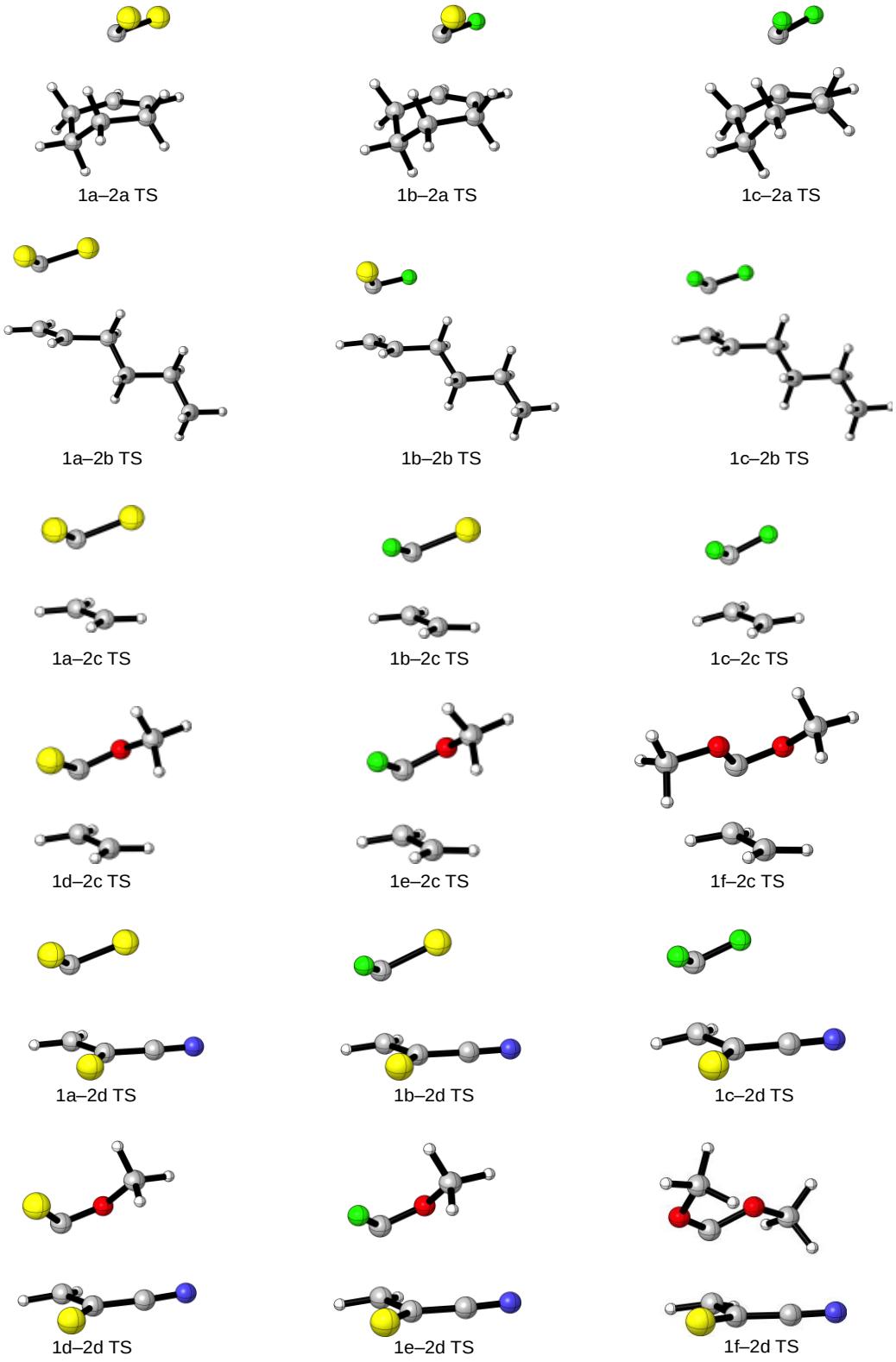

Figure 2. Optimized transition structures for the 18 cycloadditions in this study computed at the M06–2X/6–31+G(d,p) level. Geometrical parameters are given in Table 2.

Cycloadditions to cyclohexene and 1–hexene

As shown in Table 1, the cycloadditions of CCl_2 (**1a**) and CClF (**1b**) to cyclohexene (**2a**) and 1–hexene (**2b**) have negative activation energies, which are controlled by $\Delta E_i^{\ddagger}$. We found that favorable interaction energy contributes to negative ΔE at intermediate separation of the carbenes and alkenes studied here and suggests the formation of carbene–alkene precursor complexes, although the existence of these has been debated in the literature.[20–29] We have confirmed π–complexes for cycloadditions to **2a**, **2b**, and **2d** that are stabilized by 0–5 kcal mol^{-1} (ΔH^{o} = $\Delta H_{free}^{\ddagger} - \Delta H_{complex}^{\ddagger}$) relative to infinitely separated reactants; however, they are not minima on the free energy surface and thus are not expected to be experimentally stable. These computed activation energies are 6–8 kcal/mol too low when compared to activation energies determined experimentally by Moss and Krogh–Jespersen;[13] therefore, conclusions from these results should be taken with caution. An increase of 6–7 kcal mol^{-1} in the distortion energies and a decrease of 4–5 kcal mol^{-1} in the favorable (negative) interaction energies results in a substantial increase of the activation energies along the series **1a**→**1b**→**1c**. The carbene and alkene contributions to the total distortion energies for **1a** and **1b** are within ~1 kcal mol^{-1}. As for reactions of CF_2 (**1c**), distortion of the alkene is the primary cause of the increase in $\Delta E_d^{\ddagger}$, as seen in an average $\Delta\Delta E_{d,carbene}^{\ddagger}$ of 1.1 kcal mol^{-1} and $\Delta\Delta E_{d,alkene}^{\ddagger}$ of 5.1 kcal mol^{-1} relative to **1a**. Distortion of cyclohexene and 1–hexene comprises 42–72% and 40–73%, respectively, of the total distortion energy. In Table 2, the alkene bond distances, r_{13}, increase by a mere 0.02–0.03 Å from **1a**→**1b**→**1c**; therefore, C1–C3 bond elongation is not a significant contributor to $\Delta\Delta E_d^{\ddagger}$. We use angles α and β to quantify the degree of pyramidalization of the terminal alkene carbons. As shown in Table 2, α increases by 17º and β increases by 6º along the series **1a**→**1b**→**1c**. A greater extent of pyramidalization at C3 of the alkene occurs as a result of non–least motion approach in which the C2–C3 bond forms before the C2–C1 bond. We conclude that pyramidalization of the alkene carbons is the major distortion occurring at the transition state, and the change in C1–C3 bond length occurs mainly after the transition state. An increase in the values of α and β indicates progressively later transition states and greater nucleophilic character of the carbene. The distance between C2 and the midpoint of the alkene (d) as well as the forming bond distances (r_{12} and r_{23}) become shorter along the same series **1a**→**1b**→**1c**, which also supports later transition states and increasing $\Delta E_d^{\ddagger}$.

Based on the values of the carbene tilt angle γ in Table 2,[8] **1a–c** react as electrophilic carbenes toward electron–rich alkenes **2a** and **2b**. Increasing carbene LUMO energies (CCl_2: -3.74 eV; CClF: –3.39 eV; CF_2: –2.83 eV)[13] lead to decreased interaction with the π–orbitals of **2a** and **2b**, which is likely one factor that attributes to a higher $\Delta E_i^{\ddagger}$ for **1c**. However, since $\Delta E_i^{\ddagger}$ for **1a** and **1b** are essentially identical, there must be a complex interplay of factors that render this analysis of $\Delta\Delta E_i^{\ddagger}$ incomplete. An energy decomposition analysis would be required for any greater insight into the physical origins of $\Delta E_i^{\ddagger}$.

Table 2. Geometrical parameters of the cycloaddition transition structures computed at the M06–2X/6–31+G(d,p) level. Distances are in Å and angles are in degrees

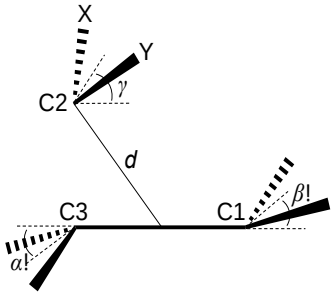

Carbene	Alkene	r_{12}	r_{23}	d	r_{13}	∠XCY	α	β	γ
CCl_2	c–Hex	2.60	2.28	2.35	1.36	108	9	1	31
CClF	c–Hex	2.41	1.99	2.10	1.37	105	18	2	35
CF_2	c–Hex	2.29	1.81	1.94	1.38	104	26	7	39
CCl_2	1–Hex	2.79	2.34	2.49	1.35	108	6	3	35
CClF	1–Hex	2.51	2.06	2.19	1.36	104	13	6	35
CF_2	1–Hex	2.39	1.81	2.01	1.38	104	23	9	41
CCl_2	C_2H_4	2.63	2.18	2.32	1.35	109	9	3	40
CClF	C_2H_4	2.46	2.00	2.14	1.36	106	15	5	39
CF_2	C_2H_4	2.37	1.84	2.00	1.37	105	22	8	44
ClCOMe	C_2H_4	2.47	1.92	2.10	1.37	113	20	4	48
FCOMe	C_2H_4	2.42	1.84	2.04	1.38	110	24	5	50
$C(OMe)_2$	C_2H_4	2.45	1.83	2.05	1.39	111	28	7	57
CCl_2	α–ClACN	2.82	2.29	2.48	1.35	110	11	5	42
CClF	α–ClACN	2.65	2.11	2.30	1.36	107	16	6	41
CF_2	α–ClACN	2.52	1.93	2.14	1.37	106	24	8	44
ClCOMe	α–ClACN	2.63	2.04	2.25	1.37	114	21	8	50
FCOMe	α–ClACN	2.56	1.96	2.17	1.38	111	24	10	49
$C(OMe)_2$	α–ClACN	2.64	2.01	2.24	1.38	112	25	11	55

Cycloadditions to ethylene

In addition to the distortion/interaction analyses for the TS that are collected in Table 1, the reaction profiles together with their decomposition into ΔE_d and ΔE_i for cycloadditions of dihalocarbenes **1a–c** and methoxycarbenes **1d–f** to ethylene (**2c**) are shown in Figure 3. Plots of ΔE_d and ΔE_i for all cycloadditions to **2c** are shown in Figures 4 and 5, respectively.

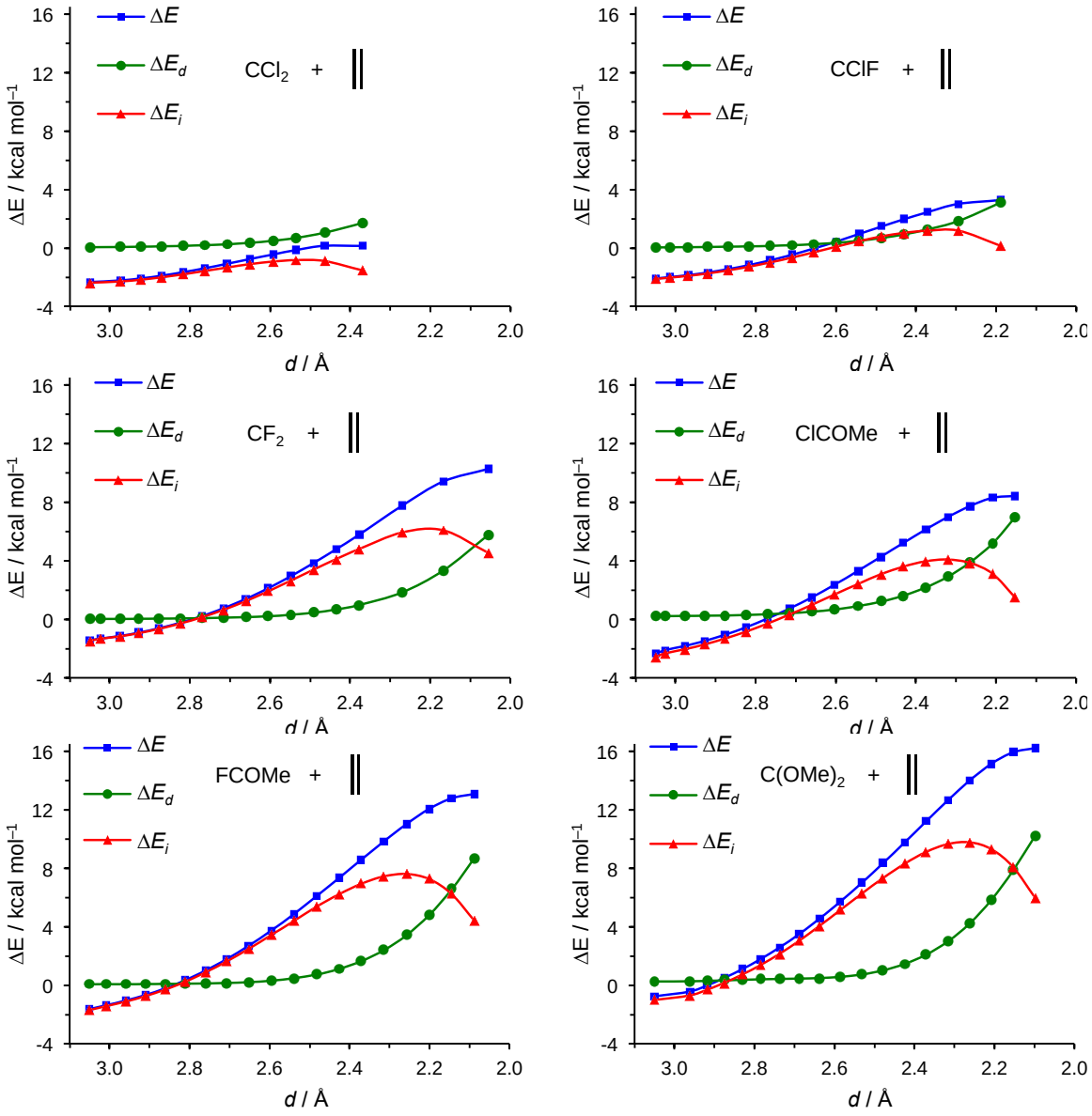

Figure 3. Distortion/interaction analysis of the (2+1) cycloaddition reaction between carbenes **1a–f** and **2c** projected onto the distance between C2 and the midpoint of ethylene (in Å). All data have been computed at the M06–2X/6–31+G(d,p) level.

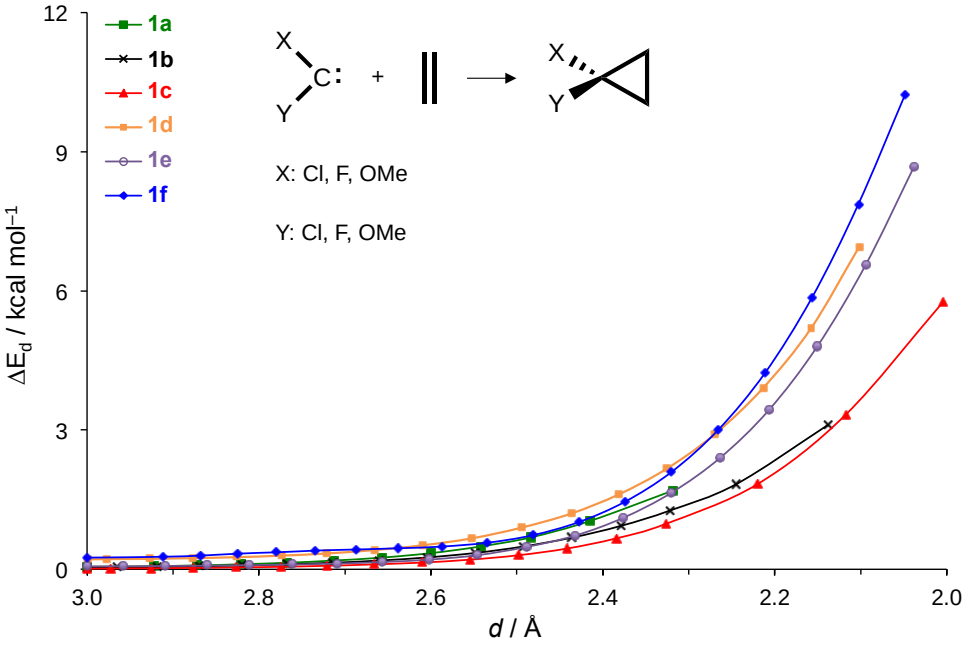

Figure 4. Distortion energy profiles of carbene cycloadditions to ethylene.

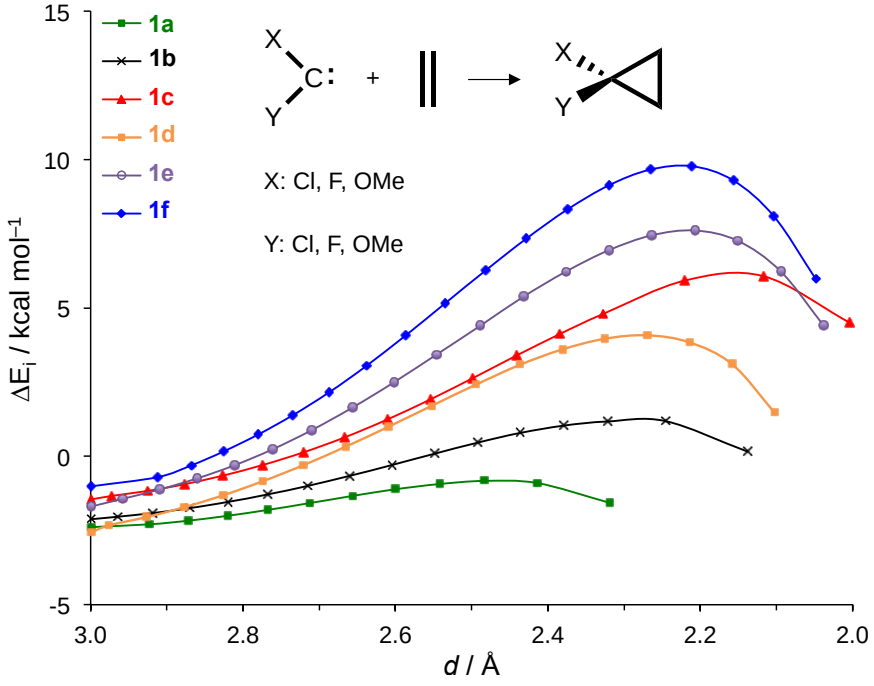

Figure 5. Interaction energy profiles of carbene cycloadditions to ethylene.

Activation energies for cycloadditions of **1a–c** and **1d–f** to **2c** increase from 0–10 and 8–16 kcal mol^{-1}, respectively. Changes in $\Delta E_d^{\ddagger}$ and $\Delta E_i^{\ddagger}$ are comparable in magnitude, and both contribute to an increase in $\Delta E^{\ddagger}$ from **1a**→**1b**→**1c** and from **1d**→**1e**→**1f**. The distortion of

ethylene comprises 51–74% of the total distortion energy. Carbene tilt angles in Table 2 indicate that **1a–c** are predominantly electrophilic and **1d–f** are predominantly nucleophilic in cycloadditions to **2c**. All interaction energies for the reactions with **2c** are positive except for that of **1a**, resulting in activation barriers greater than the inherent distortion in the transition structures. This result differs from those seen for example in 1,3-dipolar and Diels-Alder cycloadditions, where the interaction energies at the transition states are negative, i.e., favorable, in all cases such that the activation barrier is decreased relative to the distortion energy.[30] The alkyl substituents of **2a** and **2b** raise the HOMO of ethylene while the –Cl and –CN substituents of **2d** lower the LUMO of ethylene. Both of these perturbations decrease the frontier molecular orbital gaps between the carbene and alkene and lead to favorable interaction energies with respect to ethylene. Previously reported trends in HOMO and LUMO energies for these alkenes support this conclusion.[13] This trend in reactivity has been documented in the literature for other bimolecular reactions.[31-35] Houk and Ess examined cycloadditions of hydrazoic acid, an ambiphilic 1,3–dipole, to a series of substituted alkenes and found that electron–rich and electron–deficient alkenes lower the activation barriers ~2 kcal mol^{-1} compared to ethylene.[30]

From the distortion/interaction analyses in Figure 3, medium–range (d ~ 3 Å) attractive interactions exist while there is yet no distortion between the carbene and ethylene. This results in a negative ΔE relative to infinitely separated reactants and indicates formation of π-complexes, as mentioned earlier. In all cycloadditions to ethylene, there is no substantial increase in ΔE_d while d > 2.4 Å (Figure 3); therefore, the rise in ΔE along the reaction coordinate is primarily due to an increasingly destabilizing interaction between the carbene and the alkene. The early inversion of ΔE_i from destabilizing to stabilizing in **1a** is responsible for a particularly early transition state. This behavior seems to be general to pericyclic reactions as it has been observed by Bickelhaupt in (3+2) cycloadditions,[36] Alder–ene reactions,[37] and double group–transfer reactions.[38] Bickelhaupt has also pointed out that the initially destabilizing ΔE_i observed in pericyclic reactions contrasts those seen in other bimolecular reactions such as S_N2 substitution[39] and E2 elimination.[40]

Cycloadditions to α–chloroacrylonitrile

The same general increase in $\Delta E^{\ddagger}$ from **1a→1b→1c** is observed with α–chloroacrylonitrile as in additions to **2a–c** due to increased stabilization of the carbene by fluorine substituents. The distortion of α–chloroacrylonitrile (**2d**) is the dominant factor of $\Delta E_d^{\ddagger}$, comprising 71–100% of the total distortion energy in the transition state. The activation energy of **1a** addition to **2d** is negative due to a favorable interaction energy of 4.5 kcal mol^{-1} that compensates for the 1 kcal mol^{-1} distortion energy of **2d** in the transition state. The computed activation barrier of –3.2 kcal/mol for the cycloaddition of **1a** to **2d** is substantially lower than the experimentally determined value of 5.4 kcal/mol.[13] There is a dramatic increase in reactivity of **1d–f** toward **2d** as compared to **2c** ($\Delta\Delta E^{\ddagger}$ ranges from 8–15 kcal mol^{-1}). These differences are caused by large favorable changes in interaction energy and relatively small unfavorable changes in distortion energy of the **2d** series relative to **2c**: average values of $\Delta\Delta E_d^{\ddagger}$ and $\Delta\Delta E_i^{\ddagger}$ for cycloadditions of **1d–f** to **2c** and **2d** are +2.4 and –8.7 kcal mol^{-1} respectively. Cycloadditions of **1c** and **1d** to **2d**

have the same amount of distortion in the TS; thus, the higher reactivity of **1d** relative to **1c** is a result of a 5 kcal mol^{-1} difference in $\Delta E_i^{\ddagger}$.

We investigated the relationship between the distortion energies and activation energies as was done previously for other cycloaddition reactions.[41–43] Houk and Ess discovered a linear correlation between activation energy and distortion energy in the transition states for 18 1,3-dipolar cycloadditions.[30] Houk and co–workers also observed a similar correlation for 1,4-dihydrogenations and Diels–Alder cycloadditions of aromatic molecules.[41] Figure 6 shows a plot of $\Delta E^{\ddagger}$ versus $\Delta E_d^{\ddagger}$ for the cycloadditions to ethylene and α–chloroacrylonitrile. The observed correlation (r^2 = 0.95) for cycloadditions to **2c** indicates that the increasing activation barrier is a direct result of increasing distortion energy in the transition state. The cooperative increase in $\Delta E_i^{\ddagger}$ as shown in Table 1 results in the same correlation (r^2 = 0.95) between $\Delta E^{\ddagger}$ and $\Delta E_i^{\ddagger}$ for additions to **2c** (Figure S–1). Therefore, activation energies for cycloadditions of **1a–f** to **2c** are equally controlled by both $\Delta E_d^{\ddagger}$ and $\Delta E_i^{\ddagger}$. Similarly, $\Delta E_d^{\ddagger}$ and $\Delta E_i^{\ddagger}$ exert equal control of $\Delta E^{\ddagger}$ for cycloadditions of **1a–c** to **2a** and **2b** with r^2 ~ 0.95–0.99 (not shown). For cycloadditions to **2d**, there is essentially no correlation (r^2 = 0.38) between $\Delta E^{\ddagger}$ and $\Delta E_d^{\ddagger}$ for the complete carbene set; however, a correlation does exist for the dihalocarbenes **1a–c** (r^2 = 1).

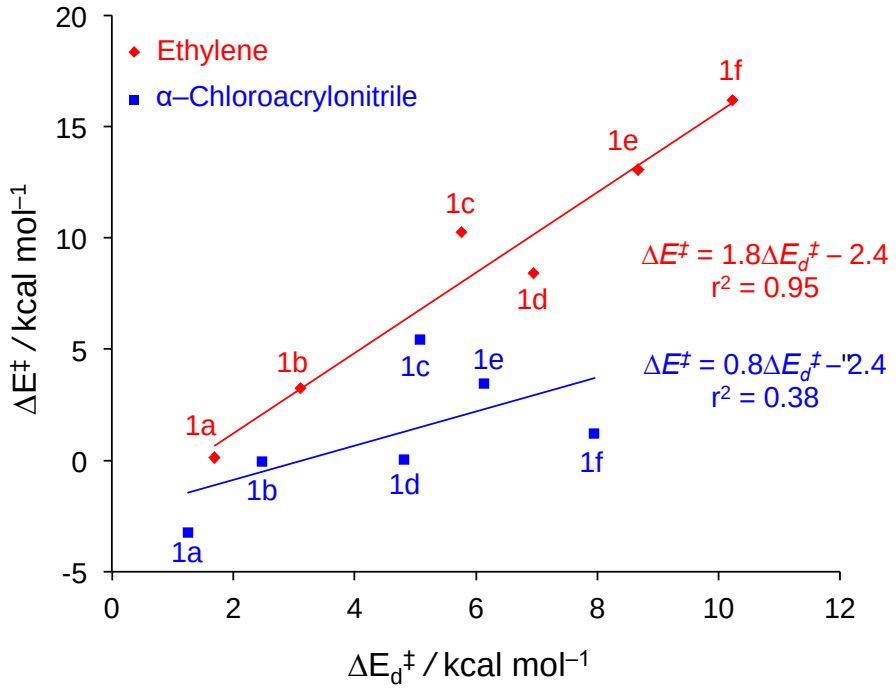

Figure 6. Plot of activation energy versus distortion energy for carbene cycloadditions to ethylene (2c; red diamonds) and α–chloroacrylonitrile (2d; blue squares).

Conclusions

Generally, it is observed that pyramidalization of the alkene carbons is the primary contributor to $\Delta E_d^{\ddagger}$ in carbene cycloadditions. When compared to dihalocarbenes **1a** and **1b**, cycloadditions of **1c** to all four alkenes show anomalously unfavorable interaction energies in the transition state. Cycloadditions of **1b** and **1c** with **2c** have essentially the same distortion energy profile, as seen in Figure 4; therefore, the higher $\Delta E^{\ddagger}$ of the latter is the result of a later transition state originating from more destabilizing ΔE_i throughout the reaction. $\Delta E_d^{\ddagger}$ is constant for the reactions of **1c** and **1d** to **2d**, so a more favorable $\Delta E_i^{\ddagger}$ relative to **1c** is responsible for the higher reactivity of **1d**. The cycloaddition of $C(OMe)_2$ to α–chloroacrylonitrile shows a $\Delta E_i^{\ddagger}$ that is more favorable than expected (**1f** + **2d**; Table 1) and contributes to a breakdown in the correlation between $\Delta E^{\ddagger}$ and $\Delta E_d^{\ddagger}/\Delta E_i^{\ddagger}$ observed for **2a–c**. These results suggest that (2+1) cycloadditions are not only distortion–controlled as are other pericyclic reactions. As represented in Figures 4 and 5, small differences in distortion energies but large differences in interaction energies control the position of the transition state and the reaction rate.

References

1. Hoffmann, R. J. Am. Chem. Soc. 1968, 90, 1475–1485. http://dx.doi.org/10.1021/ja01008a016
2. Woodward, R. B.; Hoffmann, R. *Angew. Chem. Int. Ed.* **1969**, *8*, 781–853 and references cited therein. http://dx.doi.org/10.1002/anie.196907811
3. Moore, W. R.; Moser, W. R.; LaPrade, J. E. *J. Org. Chem.* **1963**, *28*, 2200–2205. http://dx.doi.org/10.1021/jo01044a012
4. Bodor, N.; Dewar, M. J. S.; Wasson, J. S. *J. Am. Chem. Soc.* **1972**, *94*, 9095–9102. http://dx.doi.org/10.1021/ja00781a018
5. Hoffmann, R.; Hayes, D. M.; Skell, P. S. *J. Phys. Chem.* **1972**, *76*, 664–669. http://dx.doi.org/10.1021/j100649a010
6. Kollmar, H. J. *J. Am. Chem. Soc.* **1978**, *100*, 2660–2664. http://dx.doi.org/10.1021/ja00477a015
7. Joo, H.; Kraka, E.; Quapp, W.; Cremer, D. *Mol. Phys.* **2007**, *105*, 2697–2717 and references cited therein. http://dx.doi.org/10.1080/00268970701620677
8. Rondan, N. G.; Houk, K. N.; Moss, R. A. *J. Am. Chem. Soc.* **1980**, *102*, 1770–1776. http://dx.doi.org/10.1021/ja00526a002
9. Moss, R. A.; Wang, L.; Zhang, M.; Skalit, C.; Krogh–Jespersen, K. *J. Am. Chem. Soc.* **2008**, *130*, 5634–5635. http://dx.doi.org/10.1021/ja8005226 PMid:18393413

10. Moss, R. A.; Wang, L.; Krogh–Jespersen, K. *J. Am. Chem. Soc.* **2009**, *131*, 2128–2130.
http://dx.doi.org/10.1021/ja809370j
PMid:19173648
11. Moss, R. A.; Wang, L.; Zhang, M. *Org. Lett.* **2008**, *10*, 4045–4048.
http://dx.doi.org/10.1021/ol801575v
PMid:18729368
12. Moss, R. A.; Zhang, M.; Krogh–Jespersen, K. *Org. Lett.* **2010**, *12*, 3476–3479.
http://dx.doi.org/10.1021/ol1013119
PMid:20597479
13. Zhang, M.; Moss, R. A.; Thompson, J.; Krogh–Jespersen, K. *J. Org. Chem.* **2012**, *77*, 843–850.
http://dx.doi.org/10.1021/jo2023558
PMid:22204738
14. Ess, D. H.; Houk, K. N. *J. Am. Chem. Soc.* **2007**, *129*, 10646–10647.
http://dx.doi.org/10.1021/ja0734086
PMid:17685614
15. van Zeist, W.-J.; Bickelhaupt, F. M. *Org. Biomol. Chem.* **2010**, *8*, 3118–3127.
http://dx.doi.org/10.1039/b926828f
PMid:20490400
16. Zhao, Y.; Truhlar, D. G. *Theor. Chem. Account* **2008**, *120*, 215–241.
http://dx.doi.org/10.1007/s00214-007-0310-x
17. Frisch, M. J. *et al*. *Gaussian 09*, revision C–01; Gaussian, Inc.: Wallingford, CT, 2009 (see complete reference in the Supporting Information).
18. Fukui, K. *J. Phys. Chem.* **1970**, *74*, 4161–4163.
http://dx.doi.org/10.1021/j100717a029
19. Deng, L; Ziegler, T. *Int. J. Quantum Chem.* **1994**, *52*, 731–765.
http://dx.doi.org/10.1002/qua.560520406
20. Moss, R. A.; Lawrynowicz, W.; Turro, N. J.; Gould, I. R.; Cha, Y. *J. Am. Chem. Soc.* **1986**, *108*, 7028–7032.
http://dx.doi.org/10.1021/ja00282a030
21. Houk, K. N.; Rondan, N. G.; Mareda, J. *J. Am. Chem. Soc.* **1984**, *106*, 4291–4293.
http://dx.doi.org/10.1021/ja00327a052
22. Houk, K. N.; Rondan, N. G.; Mareda, J. *Tetrahedron* **1985**, *41*, 1555–1563.
http://dx.doi.org/10.1016/S0040-4020(01)96395-1
23. Turro, N. J.; Lehr, G. F.; Butcher, J. A., Jr.; Moss, R. A.; Guo, W. *J. Am. Chem. Soc.* **1982**, *104*, 1754–1756.
http://dx.doi.org/10.1021/ja00370a059
24. Moss, R. A.; Perez, L. A.; Turro, N. J.; Gould, I. R.; Hacker, N. P. *Tetrahedron Lett.* **1983**, *24*, 685-688.
http://dx.doi.org/10.1016/S0040-4039(00)81498-7
25. Gould, I. R.; Turro, N. J.; Butcher, J. A., Jr., Doubleday, C. E., Jr., Hacker, N. P.; Lehr, G. F.; Moss, R. A.; Cox, D. P.; Guo, W.; Munjal, R. C.; Perez, L. A. Fedorynski, M. *Tetrahedron*

1985, *41*, 1587–1600.
http://dx.doi.org/10.1016/S0040-4020(01)96399-9
26. Liu, M. T. H. *J. Chem. Soc., Chem. Commun.* **1985**, 982–985.
27. Liu, M. T. H.; Subramanian, R. *Tetrahedron Lett.* **1985**, *26*, 3071–3074.
http://dx.doi.org/10.1016/S0040-4039(00)98621-0
28. Tomioka, H.; Hayashi, N.; Izawa, Y.; Liu, M. T. H. *J. Am. Chem. Soc.* **1984**, *106*, 454–456.
http://dx.doi.org/10.1021/ja00314a051
29. Liu, M. T. H.; Subramanian, R. *J. Chem. Soc., Chem. Commun.* **1984**, 1062–1064.
30. Ess, D. H.; Houk, K. N. *J. Am. Chem. Soc.* **2008**, *130*, 10187–10198.
http://dx.doi.org/10.1021/ja800009z
PMid:18613669
31. Huisgen, R. In *1,3–Dipolar Cycloaddition Chemistry*; Padwa, A., Ed.; John Wiley and Sons: New York, 1984; Vol. 1 and references cited therein.
32. Houk, K. N. In *1,3–Dipolar Cycloaddition Chemistry*; Padwa, A., Ed.; John Wiley and Sons: New York, 1984; Vol. 2 and references cited therein.
33. Houk, K. N.; Sims, J.; Duke, R. E., Jr.; Strozier, R. W.; George, J. K. *J. Am. Chem. Soc.* **1973**, *95*, 7287–7301.
http://dx.doi.org/10.1021/ja00803a017
34. Houk, K. N.; Sims, J.; Watts, C. R.; Luskus, L. J. *J. Am. Chem. Soc.* **1973**, *95*, 7301–7315.
http://dx.doi.org/10.1021/ja00803a018
35. Bastide, J.; Ghandour, W. E.; Henri–Rousseau, O. *Tetrahedron Lett.* **1972**, *13*, 4225–4228.
http://dx.doi.org/10.1016/S0040-4039(01)94281-9
36. Fernandez, I.; Bickelhaupt, F. M.; Cossio, F. P. *J. Org. Chem.* **2011**, *76*, 2310–2314.
http://dx.doi.org/10.1021/jo102572x
PMid:21388217
37. Fernandez, I.; Bickelhaupt, F. M. *J. Comput. Chem.* **2012**, *33*, 509–516.
http://dx.doi.org/10.1002/jcc.22877
PMid:22144106
38. Fernandez, I.; Bickelhaupt, F. M.; Cossio, F. P. *Chem. Eur. J.* **2009**, *15*, 13022–13032.
http://dx.doi.org/10.1002/chem.200902024
PMid:19852009
39. Bento, P. A.; Bickelhaupt, F. M. *J. Org. Chem.* **2008**, *73*, 7290–7299.
http://dx.doi.org/10.1021/jo801215z
PMid:18690745
40. Bickelhaupt, F. M. *J. Comput. Chem.* **1999**, *20*, 114–128.
http://dx.doi.org/10.1002/(SICI)1096-987X(19990115)20:1<114::AID-JCC12>3.0.CO;2-L
41. Hayden, A. E.; Houk, K. N. *J. Am. Chem. Soc.* **2009**, *131*, 4084–4089.
http://dx.doi.org/10.1021/ja809142x
PMid:19256544
42. Liang, Y.; Mackey, J. L.; Lopez, S. A.; Liu, F.; Houk, K. N. *J. Am. Chem. Soc.* **2012**, *134*, 17904–17907.
http://dx.doi.org/10.1021/ja809142x

PMid:19256544
43. Lopez, S. A.; Houk, K. N. *J. Org. Chem.* **2013**, *78*, 1778–1783.
http://dx.doi.org/10.1021/jo301267b
PMid:22764840

